From spatial symmetry to the numbers of Raman- and infrared-active vibrations in single-walled nanotubes*

Ofir E. Alon†
Department of Chemistry, Technion-Israel Institute of Technology, Haifa 32000, Israel

Abstract

By analyzing the point groups of the nonsymmorphic rod-groups of single-walled carbon nanotubes (CNT's) we show that all achiral CNT's possess only 8 Raman-active and 3 infrared-active phonon modes. This is in *contrast* to previously predicted 15-16 and 7-8 active modes, respectively. Similarly, we find that all chiral CNT's have 14 (instead of 15) Raman-active and 6 (instead of 9) infrared-active phonon modes. Lowering the spatial symmetry of CNT's, by considering single-walled boron-nitride nanotubes (BNT's), leads to additional active modes. However, unlike the situation for achiral CNT's, we find that zigzag BNT's possess almost twice Raman- and infrared-active vibrations as armchair BNT's.

I. INTRODUCTION

Since their discovery by Iijima in 1991 [1], CNT's have attracted enormous attention of both experimentalists and theoreticians for their novel properties and potential applications (see, e.g., Refs. [2,3] and references therein). CNT's are a synthesized allotropic form of carbon (see Ref. [4] for review of their physical properties). Single-walled CNT's (hereafter, CNT's), to which we will restrict our attention, can be viewed as cylinders made of graphite sheets (graphene). The infinite order, two-dimensional (2D) translational symmetries of the hexagonal net can transform into various finite order symmetries once the graphene plane is transformed (rolled) into the CNT cylinder. The order and character of the resulting symmetries depend on the way the graphene boundaries are connected with each other to form the cylinder.

---

*Lecture to be presented at the N&N2001 Workshop, Frascati, Itali, 25-27 October.

†Present address: Physikalisch-Chemisches Institut, Theoretische Chemie, Universität Heidelberg, Im Neuenheimer Feld 229, D-69120 Heidelberg, Germany. E-mail: ofir@tc.pci.uni-heidelberg.de

In Fig. (1), the classification according to the pair of indices (n, m), representing different CNT's, is illustrated. The (n, m) CNT is formed by rolling the graphene sheet along the chiral vector

$$\mathbf{C_h} = n\mathbf{a_1} + m\mathbf{a_2} \tag{1}$$

($\mathbf{a_1}$ and $\mathbf{a_2}$ are the two primitive vectors of the honeycomb lattice), such that its origin O and its end point O' coincide on the CNT. If the graphene sheet is rolled along the $n\mathbf{a_1}$ direction then an achiral zigzag CNT, classified by the pair of indices $(n, 0)$, is formed. If the graphene sheet is rolled along the $n(\mathbf{a_1} + \mathbf{a_2})$ direction then an achiral armchair CNT, classified by the pair of indices (n, n), is formed. In all other cases, i.e. whenever $0 < m < n$, a chiral CNT is formed.

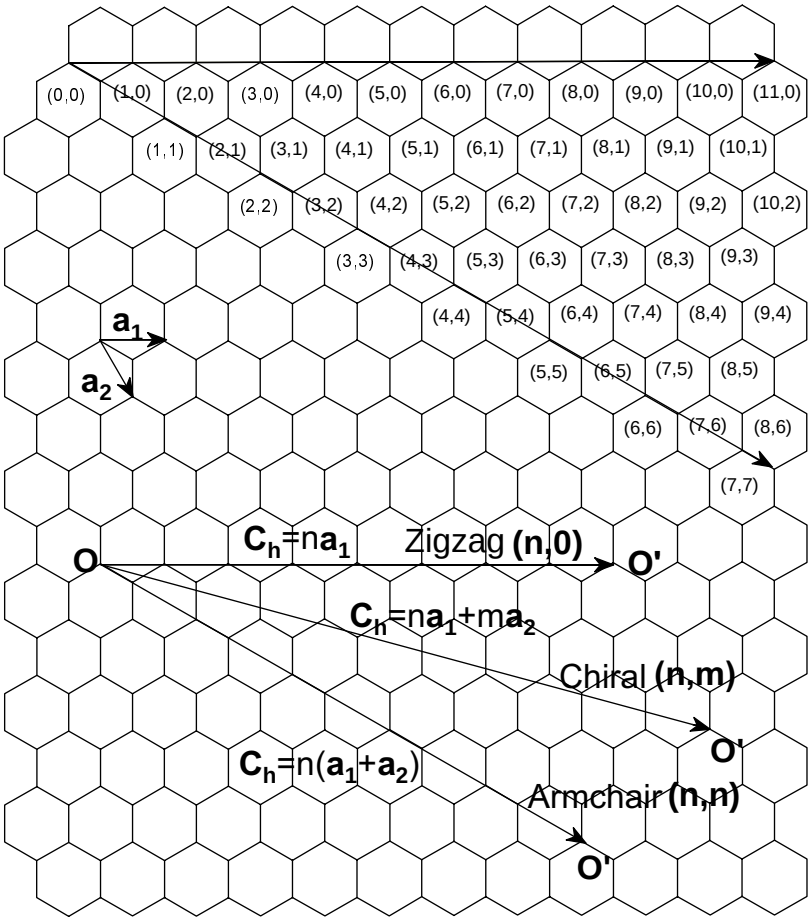

Figure 1: Classification of CNT's according to the pair of indices (n, m). $\mathbf{a_1}$ and $\mathbf{a_2}$ are the two primitive vectors of the honeycomb lattice. The chiral vectors, $\mathbf{C}_\mathrm{h} = \mathbf{OO}'$, are shown for zigzag, chiral and armchair CNT's.

The primitive translation vector of the CNT *unit cell*, $\mathbf{T_z}$, is given by

$$\mathbf{T_z} = \frac{1}{d_R}\left[(2m+n)\,\mathbf{a_1} - (2n+m)\,\mathbf{a_2}\right], \tag{2}$$

where d_R is the greatest common divisor of $2n+m$ and $2m+n$ [4]. From the size of the unit cell, which is defined by the orthogonal vectors $\mathbf{T_z}$ and $\mathbf{C_h}$, we can readily find the number of hexagons per unit cell,

$$N = \frac{2\left(m^2+mn+n^2\right)}{d_R}. \tag{3}$$

Note that each hexagon contains two carbon atoms.

Boron-nitride nanotubes (BNT's) are recently synthesized (Chopra *et al.* [5], Yu *et al.* [6]) novel type of materials, combining stable insulating properties (Rubio *et al.* [7], *et al.* Blase [8]) and high strength (Chorpa and Zettl [9]). Owing to the subset relation between the plane-groups of 2D hexagonal boron-nitride and graphite nets

$$p3m1 \subseteq p6mm, \tag{4}$$

single-walled BNT's (hereafter, BNT's) are characterized by the pair of indices n and m as CNT's do: $(n, m = n)$-armchair, $(n, m = 0)$-zigzag and $(n, 0 < m < n)$-chiral. Thus, the (n, m) BNT and CNT possess the same lattice period $\mathbf{T_z}$ and number N of hexagons within their unit cells. Ab-initio studies of the spatial *structure* of BNT's have predicted the buckling of B-N bonds, i.e., the formation of concentric inner "B-cylinder" and outer "N-cylinder" (Blase *et al.* [8], Menon and Srivastava [10]).

II. ACTIVE PHONONS IN SINGLE-WALLED CARBON NANOTUBES

The classification of CNT symmetries is an essential stage in predicting their physical properties, among which are active infrared (IR) and Raman vibrations (see Ref. [4] and references therein). For example, there are 15-16 Raman-active phonon modes predicted for infinitely long armchair CNT's [4], with frequencies up to about 1600 cm^{-1}. Of them 7 modes are intense (in the low and high frequency zones), while the rest (in the intermediate frequency zone) have no intensity for infinite nanotubes (Saito *et al.* [11]), but do have some intensity for finite nanotubes (Saito *et al.* [12]). Such predictions have clear fingerprints in Raman scattering experiments from CNT ropes (Rao *et al.* [13], Journet *et al.* [14]).

Until very recently [15], the determination of optically-active phonon modes in achiral CNT's has been performed with symmorphic rod-groups (Dresselhaus and co-workers; see Ref. [4] and references therein). In order to account for the inversion symmetry operation, unit cells possessing the point-groups $\mathcal{D}_{nh}$ or $\mathcal{D}_{nd}$ for even or odd n's, respectively, were chosen for the $(n, 0)$-zigzag and (n, n)-armchair CNT's. However, achiral CNT's possess in addition a screw-axis of order $2n$ and n glide planes (Damnjanović *et al.* [16]). Due to these operations the symmetry of achiral CNT's is described by non-symmorphic rod-groups, as elucidated recently by Damnjanović *et al.* [16]. We report here the result of our recent study [15], showing that this has a dramatic effect on vibrational spectra in achiral CNT's. Especially, we show that armchair CNT's possess only 8 Raman-active vibrations, which corroborates the recent experimental data [13,14].

A. Achiral carbon nanotubes

Consider the achiral CNT's possessing the rotation axis of order n, that is the $(n,0)$-zigzag or (n,n)-armchair CNT's.

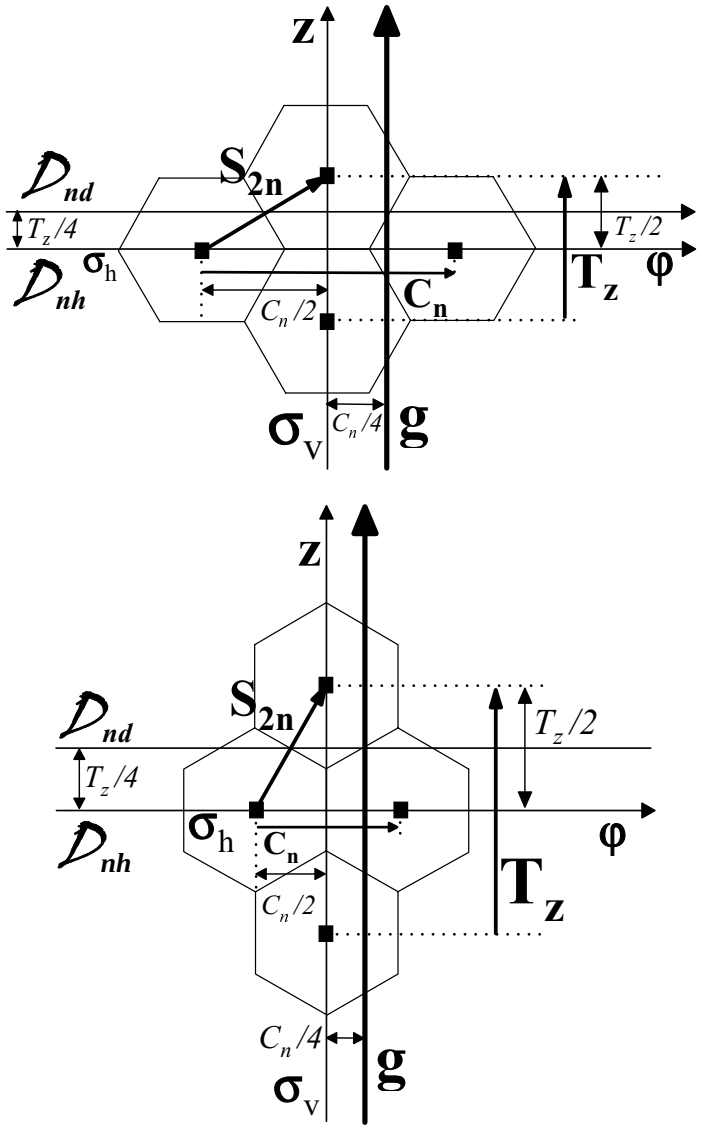

Figure 2: 2D projection of various symmetries in achiral CNT's (armchair segment - top; zigzag segment - bottom): $\mathbf{T_z}$ is the primitive translation; $\mathbf{S_{2n}}$ is the screw axis with non-primitive translation and rotation, denoted by $T_z/2$ and $C_n/2$, respectively; $\mathbf{g}$ is a glide plane; $\mathcal{D}_{nh}|_{z=0}$ and $\mathcal{D}_{nd}|_{z=\frac{T_z}{4}}$ stand for the corresponding point-group operations, among which $\sigma_\mathbf{h}$, $\sigma_\mathbf{v}$ and $\mathbf{C_n}$ are denoted. Note the $T_z/4$ shift between $\mathcal{D}_{nh}|_{z=0}$ and $\mathcal{D}_{nd}|_{z=\frac{T_z}{4}}$, that coexist in all achiral CNT's.

The non-symmorphic rod-group [16] describing the achiral CNT's with index n can be

decomposed in the following manner (the 13-th family of rod-groups [17]),

$$\begin{aligned}\mathcal{G}[n] = \mathcal{L}_{T_z} \times \mathcal{D}_{nh} \times [\mathbf{E} \oplus \mathbf{S_{2n}}] = \mathcal{L}_{T_z} \times \mathcal{D}_{nd} \times [\mathbf{E} \oplus \mathbf{S_{2n}}] = \\ \mathcal{L}_{T_z} \times \left[\mathcal{D}_{nh}|_{z=0} \oplus \left(\mathcal{D}_{nd}|_{z=\frac{T_z}{4}} \ominus \mathcal{C}_{nv}\right) \oplus \mathcal{C}_{nv} \times \mathbf{S_{2n}}\right], \end{aligned} \tag{5}$$

where the reference point $z = 0$ denotes the crossing of horizontal, $\sigma_{\mathbf{h}}$, and vertical, $\sigma_{\mathbf{v}}$, reflection planes (see Fig. (2)). $\mathcal{L}_{T_z}$ is the 1D translation group with the primitive translation $T_z = |\mathbf{T_z}|$. $\mathbf{E}$ is the identity operation. The screw axis $\mathbf{S_{2n}} = \left(z \to z + \frac{T_z}{2}, \varphi \to \varphi + \frac{\pi}{n}\right)$ involves the lattice smallest non-primitive translation and rotation. The subtraction of the point group $\mathcal{C}_{nv}$ in Eq. (5) reflects the set relation $\mathcal{D}_{nh}|_{z=0} \cap \mathcal{D}_{nd}|_{z=\frac{T_z}{4}} = \mathcal{C}_{nv}$ valid for all n's. The glide plane $\mathbf{g}$ is also presented in Fig. (2). It fulfills the multiplication relation $\mathbf{g} = \mathbf{S_{2n}}\sigma_{\mathbf{v}}$. The existence of n distinct glide planes in $\mathcal{G}[n]$ stems from the last term in Eq. (5).

The point-group of the rod-group, $\mathcal{G}_0[n]$, is obtained by setting all translations (including the non-primitive ones) in $\mathcal{G}[n]$ equal to zero. From Eq. (5) we obtain,

$$\mathcal{G}_0[n] = \mathcal{D}_{nh} \times [\mathbf{E} \oplus C_{2n}] = \mathcal{D}_{nd} \times [\mathbf{E} \oplus C_{2n}] = \mathcal{D}_{2nh}, \tag{6}$$

where $C_{2n} = \left(\varphi \to \varphi + \frac{\pi}{n}\right)$ is the rotation embedded in $\mathbf{S_{2n}}$.

Aiming at characterizing the symmetries of phonons at the $\Gamma(k=0)$-point, we would like to discuss the irreducible representations (irrep's) of $\mathcal{G}[n]$ at Γ. As known from the theory of space-groups [18], these irrep's are in a one-to-one correspondence with the irrep's of the factor-group of the wave vector $k = 0$, which is isomorphic to $\mathcal{G}_0[n] = \mathcal{D}_{2nh}$. Recall that the character table of $\mathcal{D}_{2nh}$ possesses $2n + 6$ irrep's [19],

$$\Gamma_{\mathcal{D}_{2nh}} = A_{1g} \oplus A_{2g} \oplus B_{1g} \oplus B_{2g} \oplus A_{1u} \oplus A_{2u} \oplus B_{1u} \oplus B_{2u} \oplus \sum\nolimits_{j=1}^{n-1} \{E_{jg} \oplus E_{ju}\}. \tag{7}$$

Next, we would like to determine the symmetries of the $6N$ phonon modes at the Γ-point and how many modes are Raman- or IR-active. Recall that for achiral CNT's $N = 2n$. At this point we have to differentiate between $(n, 0)$-zigzag and (n, n)-armchair CNT's, due to the differences in atom-arrangements inside their unit cells. The $6N$ phonon modes transform according to the following irrep's for zigzag CNT's:

$$\begin{aligned}\Gamma_{6N}^{zig,n\in\text{evens}} &= \Gamma_{\text{a}}^{zig} \otimes \Gamma_{\text{v}} = 2A_{1g} \oplus A_{2g} \oplus 2B_{1g} \oplus B_{2g} \oplus A_{1u} \oplus \\ &\oplus 2A_{2u} \oplus B_{1u} \oplus 2B_{2u} \oplus \sum\nolimits_{j=1}^{n-1} \{3E_{jg} \oplus 3E_{ju}\} \\ \\ \Gamma_{6N}^{zig,n\in\text{odds}} &= \Gamma_{\text{a}}^{zig} \otimes \Gamma_{\text{v}} = 2A_{1g} \oplus A_{2g} \oplus B_{1g} \oplus 2B_{2g} \oplus A_{1u} \oplus \\ &\oplus 2A_{2u} \oplus 2B_{1u} \oplus B_{2u} \oplus \sum\nolimits_{j=1}^{n-1} \{3E_{jg} \oplus 3E_{ju}\}, \end{aligned} \tag{8}$$

where,

$$\begin{aligned}\Gamma_{\text{a}}^{zig,n\in\text{evens}} &= A_{1g} \oplus B_{1g} \oplus A_{2u} \oplus B_{2u} \oplus \sum\nolimits_{j=1}^{n-1} \{E_{jg} \oplus E_{ju}\} \\ \Gamma_{\text{a}}^{zig,n\in\text{odds}} &= A_{1g} \oplus B_{2g} \oplus A_{2u} \oplus B_{1u} \oplus \sum\nolimits_{j=1}^{n-1} \{E_{jg} \oplus E_{ju}\}, \end{aligned} \tag{9}$$

stand for the reducible representations of the carbon-atom positions inside the unit cells. $\Gamma_{\rm v} = A_{2u} \oplus E_{1u}$ is the vector representation. Similarly, the $6N$ phonon modes for armchair CNT's transform according to the following irrep's:

$$\begin{aligned}\Gamma_{6N}^{arm,n\in\text{evens}} = \Gamma_{\rm a}^{arm} \otimes \Gamma_{\rm v} = 2A_{1g} \oplus 2A_{2g} \oplus 2B_{1g} \oplus 2B_{2g} \oplus A_{1u} \oplus A_{2u} \oplus B_{1u} \oplus B_{2u} \oplus \\ \oplus 2E_{1g} \oplus 4E_{2g} \oplus 2E_{3g} \oplus 4E_{4g} \oplus \ldots \oplus \left(3 + (-1)^{n-1}\right) E_{(n-1)g} \oplus \\ \oplus 4E_{1u} \oplus 2E_{2u} \oplus 4E_{3u} \oplus 2E_{4u} \oplus \ldots \oplus \left(3 - (-1)^{n-1}\right) E_{(n-1)u}\end{aligned}$$

$$\begin{aligned}\Gamma_{6N}^{arm,n\in\text{odd}} = \Gamma_{\rm a}^{arm} \otimes \Gamma_{\rm v} = 2A_{1g} \oplus 2A_{2g} \oplus B_{1g} \oplus B_{2g} \oplus A_{1u} \oplus A_{2u} \oplus 2B_{1u} \oplus 2B_{2u} \oplus \\ \oplus 2E_{1g} \oplus 4E_{2g} \oplus 2E_{3g} \oplus 4E_{4g} \oplus \ldots \oplus \left(3 + (-1)^{n-1}\right) E_{(n-1)g} \oplus \\ \oplus 4E_{1u} \oplus 2E_{2u} \oplus 4E_{3u} \oplus 2E_{4u} \oplus \ldots \oplus \left(3 - (-1)^{n-1}\right) E_{(n-1)u}, \qquad (10)\end{aligned}$$

where,

$$\begin{aligned}\Gamma_{\rm a}^{arm,n\in\text{even}} &= A_{1g} \oplus A_{2g} \oplus B_{1g} \oplus B_{2g} \oplus 2\sum\nolimits_{j=2l}^{n-1} E_{jg} \oplus 2\sum\nolimits_{j=2l-1}^{n-1} E_{ju} \\ \Gamma_{\rm a}^{arm,n\in\text{odd}} &= A_{1g} \oplus A_{2g} \oplus B_{1u} \oplus B_{2u} \oplus 2\sum\nolimits_{j=2l}^{n-1} E_{jg} \oplus 2\sum\nolimits_{j=2l-1}^{n-1} E_{ju}, \qquad (11)\end{aligned}$$

stand for the reducible representations of the carbon-atom positions inside the unit cells. Of these modes, the ones that transform according to $\Gamma_{\rm t} = A_{1g} \oplus E_{1g} \oplus E_{2g}$ (the tensor representation) or $\Gamma_{\rm v}$ are Raman- or IR-active, respectively. Out of the $6N$ phonon modes, four (which transform as $\Gamma_{\rm v}$ and $\Gamma_{R_z} = A_{2g}$) have vanishing frequencies [4,20]. Consequently, the symmetries and numbers of optically-active phonon modes in zigzag CNT's (with either odd or even index n) are given by:

$$\Gamma_{\rm Raman}^{zig} = 2A_{1g} \oplus 3E_{1g} \oplus 3E_{2g} \implies n_{\rm Raman}^{zig} = 8\,, \qquad (12)$$

$$\Gamma_{\rm IR}^{zig} = A_{2u} \oplus 2E_{1u} \implies n_{\rm IR}^{zig} = 3\,, \qquad (13)$$

and in armchair CNT's (with either odd or even index n):

$$\Gamma_{\rm Raman}^{arm} = 2A_{1g} \oplus 2E_{1g} \oplus 4E_{2g} \implies n_{\rm Raman}^{arm} = 8\,, \qquad (14)$$

$$\Gamma_{\rm IR}^{arm} = 3E_{1u} \implies n_{\rm IR}^{arm} = 3. \qquad (15)$$

Thus, the numbers of Raman- and IR-active phonon modes are fixed for all zigzag and armchair CNT's, as previously predicted by Dresselhaus and co-workers using the *subgroup* point-groups $\mathcal{D}_{nh}, \mathcal{D}_{nd} \subseteq \mathcal{D}_{2nh}$ (see Ref. [4] and references therein). However, due to the higher rod-group and factor-group symmetries there are much fewer active modes: 8 (Raman) and 3 (IR), instead of 15-16 and 7-8, respectively [4]. These findings corroborates the recent experimental data (see Refs. [13,14]) and theoretical predictions of Raman-line intensities (Refs. [11,12]), where only 7 intense lines were identified for armchair CNT's. For this, examine the atomic-displacements of the 7 intense Raman-active modes of the $(10, 10)$-armchair CNT (see Fig 2 in Ref. [13], or Fig. 10.6 in Ref. [4]). This reveals that they transform according to $\Gamma_{\rm t}$, not only with respect to the lower-symmetry $\mathcal{D}_{10h}$ point-group, but also with respect to the higher-symmetry $\mathcal{D}_{20h}$ factor-group. In other words, these 7 out of 16 modes (frequencies) are among the 8 modes which we predict to be Raman-active, on the basis of the higher non-symmorphic rod-group symmetry identified in armchair CNT's!

B. Chiral carbon nanotubes

Next, we would like to discuss the number of Raman- and IR-active vibrations in chiral CNT's. Until very recently [15], the determination of optically-active phonon modes in chiral CNT's has been performed with commutative non-symmorphic rod-groups (Dresselhaus and co-workers; see Ref. [4] and references therein). The point-group of the rod-group of the (n,m)-chiral CNT had been shown to be $\mathcal{C}_N$, where N is given in Eq. (3). Recently, chiral CNT's were shown to possess in addition perpendicular C_2 axes (Damnjanović *et al.* [16]). The existence of these "overlooked" symmetry operations constitute the geometrical proof that chiral CNT's possess the structure of non-commutative non-symmorphic rod-groups [16].

The non-symmorphic rod-group describing the (n,m)-chiral CNT can be decomposed as follows (the 5-th family of rod-groups [17]),

$$\mathcal{G}[N] = \mathcal{L}_{T_z} \times \mathcal{D}_d \times \left[\sum_{j=0}^{\frac{N}{d}-1} \mathbf{S}^{\mathbf{j}}_{\frac{\mathbf{N}}{\mathbf{d}}} \right] = \mathcal{L}_{T_z} \times \mathcal{D}_1 \times \left[\sum_{j=0}^{N-1} \mathbf{S}^{\mathbf{j}}_{\mathbf{N}} \right]. \tag{16}$$

d is the greatest common divisor of n and m. $\mathbf{S}_{\frac{\mathbf{N}}{\mathbf{d}}}$ and $\mathbf{S_N}$ are screw-axis operations with the orders of $\frac{N}{d}$ and N, respectively. The point-group of the rod-group is readily obtained from Eq. (16),

$$\mathcal{G}_0[N] = \sum_{j=0}^{\frac{N}{d}-1} C^j_{\frac{N}{d}} \times \mathcal{D}_d = \sum_{j=0}^{N-1} C^j_N \times \mathcal{D}_1 = \mathcal{D}_N. \tag{17}$$

where $C_{\frac{N}{d}} = \left(\varphi \to \varphi + \frac{2d\pi}{N}\right)$ and $C_N = \left(\varphi \to \varphi + \frac{2\pi}{N}\right)$ are the rotations embedded in $\mathbf{S}^{\mathbf{j}}_{\frac{\mathbf{N}}{\mathbf{d}}}$ and $\mathbf{S_N}$, respectively. As has been shown recently [15], this higher symmetry ($\mathcal{D}_N \supseteq \mathcal{C}_N$) leads to the reduction of the number of optically-active phonon modes in chiral CNT's.

Analogously to the treatment given above for achiral CNT's, we would like to discuss the irrep's of the factor-group of the wave vector $k = 0$, being $\mathcal{D}_N$ for chiral CNT's. Recall that the character table of $\mathcal{D}_N$ possesses $\frac{N}{2} + 3$ (N is always even for CNT's) irrep's [19],

$$\Gamma_{\mathcal{D}_N} = A_1 \oplus A_2 \oplus B_1 \oplus B_2 \oplus \sum_{j=1}^{\frac{N}{2}-1} E_j. \tag{18}$$

The $6N$ phonon modes transform according to the following irrep's:

$$\Gamma^{ch}_{6N} = \Gamma^{ch}_{\mathrm{a}} \otimes \Gamma_{\mathrm{v}} = 3A_1 \oplus 3A_2 \oplus 3B_1 \oplus 3B_2 \oplus \sum_{j=1}^{\frac{N}{2}-1} 6E_j, \tag{19}$$

where

$$\Gamma^{ch}_{\mathrm{a}} = A_1 \oplus A_2 \oplus B_1 \oplus B_2 \oplus \sum_{j=1}^{\frac{N}{2}-1} 2E_j, \tag{20}$$

stand for the reducible representation of the carbon-atom positions inside the unit cell. $\Gamma_{\mathrm{v}} = A_2 \oplus E_1$ is the vector representation. Of these modes, the ones that transform according to $\Gamma_{\mathrm{t}} = A_1 \oplus E_1 \oplus E_2$ and/or Γ_{v} are Raman- and/or IR-active, respectively. Four of the $6N$ phonon-modes, those which transform as Γ_{v} and $\Gamma_{R_z} = A_2$, have vanishing frequencies

[4,20]. Consequently, the symmetries and numbers of optically-active phonon modes are given by:

$$\Gamma^{ch}_{\rm Raman} = 3A_1 \oplus 5E_1 \oplus 6E_2 \implies n^{ch}_{\rm Raman} = 14\,, \tag{21}$$

$$\Gamma^{ch}_{\rm IR} = A_2 \oplus 5E_1 \implies n^{ch}_{\rm IR} = 6\,. \tag{22}$$

Thus, the numbers of Raman- and IR-active phonon modes is independent of the chiral CNT indices, (n, m), as previously predicted by Dresselhaus and co-workers (see Ref. [4] and references therein) using the *subgroup* factor-group $\mathcal{C}_N \subseteq \mathcal{D}_N$. However, due to the higher rod-group and factor-group symmetries, fewer modes are active: 14 (Raman) and 6 (IR), instead of 15 and 9, respectively [4].

III. ACTIVE PHONONS IN SINGLE-WALLED BORON-NITRIDE NANOTUBES

In contrast to CNT [4], the classification of BNT spatial *symmetries* has been completed only very recently [21,22]. The profound implication of the symmetry properties of BNT's on physical effects can be seen in the recent work of Král *et al.* [23], who predicted non-centrosymmetry- and polarity-based photogalvanic effects in BNT's. More specifically, the direction of the induced photocurrent was shown to depend on the BNT chirality. However, *all* armchair BNT's are *centrosymmetric*. Nevertheless, and in contrast to 2D and 3D centrosymmetric and polar crystalline materials, they (should) exhibit the azimuthal photocurrents predicted in Ref. [23]. Here we report the result of our recent study [22], determining the numbers of Raman- and infrared-active vibrations in BNT's and comparing them to those in CNT's.

A. Armchair and zigzag boron-nitride nanotubes

Let us consider first the achiral BNT's with the rotation axis of order n, that is the (n, n)-armchair (Fig. (3)) and $(n, 0)$-zigzag (Fig. (4)) BNT's. Unlike the situation for CNT's, they do not possess the same symmetry operations [21,22], owing to the lower symmetry described in Eq. (4). Nevertheless, they still possess symmetries of non-symmorphic rod-groups because the screw-axis $\mathbf{S_{2n}}$ "survives" this symmetry lowering (see Figs. (3) and (4)). More specifically, the (n, n)-armchair BNT possesses *horizontal* planes (see Fig. (3)). The lack of C_2 axes (recall that there are no C_2 axes in $p3m1$) leads to the absence of vertical planes in this case. Consequently, the $\mathcal{D}_{nh}$ and $\mathcal{D}_{nd}$ point-groups in armchair CNT's (see Fig. (2(top)) and Eq. (5)) reduce to $\mathcal{C}_{nh}$ and $\mathcal{S}_{2n}$, respectively (see Fig. (3)). The converse is true for the $(n, 0)$-zigzag BNT, which has *vertical* planes (see Fig. (4)), but no horizontal ones. Consequently, both $\mathcal{D}_{nh}$ and $\mathcal{D}_{nd}$ point-groups in zigzag CNT's (see Fig. (2(bottom)) and Eq. (5)) reduce to $\mathcal{C}_{nv}$ (see Fig. (4)). Therefore, the non-symmorphic rod-group describing the (n, n)-armchair BNT with (either odd or even) index n can be decomposed in the following manner (the 4-th family of rod-groups [17]),

$$\mathcal{G}^{arm}[n] = \mathcal{L}_{T_z} \times \mathcal{C}_{nh} \times [\mathbf{E} \oplus \mathbf{S_{2n}}] = \mathcal{L}_{T_z} \times \mathcal{S}_{2n} \times [\mathbf{E} \oplus \mathbf{S_{2n}}] = \mathcal{L}_{T_z} \times \left[\mathcal{C}_{nh}|_{z=0} \oplus \left(\mathcal{S}_{2n}|_{z=\frac{T_z}{4}} \ominus \mathcal{C}_n\right) \oplus \mathcal{C}_n \times \mathbf{S_{2n}}\right]. \quad (23)$$

The reference point $z = 0$ denotes the crossing of horizontal reflection plane, $\sigma_{\mathbf{h}}$, and the n-fold rotation axis, $\mathbf{C_n}$ (see Fig. (3)). The subtraction of the point group $\mathcal{C}_n$ in Eq. (23) reflects the set relation $\mathcal{C}_{nh}|_{z=0} \cap \mathcal{S}_{2n}|_{z=\frac{T_z}{4}} = \mathcal{C}_n$ valid for all n's. Note that while $p3m1$ does not possess the inversion symmetry, $\mathcal{G}^{arm}[n]$ possess this symmetry! In addition, let us point out that the buckling of B-N bonds [8,10] has no effect on the spatial symmetries of BNT's because the B and N atoms form two concentric cylinders [10] in the BNT's. The point-group of the rod-group is readily obtained from Eq. (23),

$$\mathcal{G}_0^{arm}[n] = \mathcal{C}_{nh} \times [\mathbf{E} \oplus C_{2n}] = \mathcal{S}_{2n} \times [\mathbf{E} \oplus C_{2n}] = \mathcal{C}_{2nh}. \quad (24)$$

Similarly, the non-symmorphic rod-group describing the $(n, 0)$-zigzag BNT with (either odd or even) index n can be decomposed in the following manner (the 8-th family of rod-groups [17]),

$$\mathcal{G}^{zig}[n] = \mathcal{L}_{T_z} \times \mathcal{C}_{nv} \times [\mathbf{E} \oplus \mathbf{S_{2n}}]. \quad (25)$$

Note that the glide planes in zigzag CNT's (see Fig. (2(bottom)) and Eq. (5)) are preserved in zigzag BNT's (see Fig. (4) and Eq. (25)). The point-group of the rod-group is readily obtained from Eq. (25),

$$\mathcal{G}_0^{zig}[n] = \mathcal{C}_{nv} \times [\mathbf{E} \oplus C_{2n}] = \mathcal{C}_{2nv}. \quad (26)$$

In order to determine the symmetries (at the Γ-point) of the $6N$ phonon modes in armchair BNT's and how many modes are Raman- or IR-active we have to associate them with the irrep's of $\mathcal{G}_0^{arm}[n] = \mathcal{C}_{2nh}$. Recall that the character table of $\mathcal{C}_{2nh}$ possesses $4n$ irrep's [19],

$$\Gamma_{\mathcal{C}_{2nh}} = A_g \oplus B_g \oplus A_u \oplus B_u \oplus \sum_{j=1}^{n-1} \left\{E_{jg}^{\pm} \oplus E_{ju}^{\pm}\right\}. \quad (27)$$

The $6N$ phonon modes transform according to the following irrep's:

$$\begin{aligned}\Gamma_{6N}^{arm} &= \Gamma_{\mathrm{a}}^{arm} \otimes \Gamma_{\mathrm{v}} = 4A_g \oplus 2B_g \oplus 2A_u \oplus 4B_u \oplus \\ &\oplus 2E_{1g}^{\pm} \oplus 4E_{2g}^{\pm} \oplus 2E_{3g}^{\pm} \oplus \ldots \oplus \left(3 + (-1)^{n-1}\right) E_{(n-1)g}^{\pm} \oplus \\ &\oplus 4E_{1u}^{\pm} \oplus 2E_{2u}^{\pm} \oplus 4E_{3u}^{\pm} \oplus \ldots \oplus \left(3 - (-1)^{n-1}\right) E_{(n-1)u}^{\pm}, \end{aligned} \quad (28)$$

where,

$$\Gamma_{\mathrm{a}}^{arm} = 2\left(A_g \oplus B_u \oplus \sum_{j=2l}^{n-1} E_{jg}^{\pm} \oplus \sum_{j=2l-1}^{n-1} E_{ju}^{\pm}\right), \quad (29)$$

stands for the reducible representations of the B and N atom positions inside the unit cell. The prefactor of 2 in $\Gamma_{\mathrm{a}}^{arm}$, Eq. (29), reflects the two equivalent and disjoint sub-lattices made by the B and N atoms in the BNT's. $\Gamma_{\mathrm{v}} = A_u \oplus E_{1u}^{\pm}$ is the vector representation.

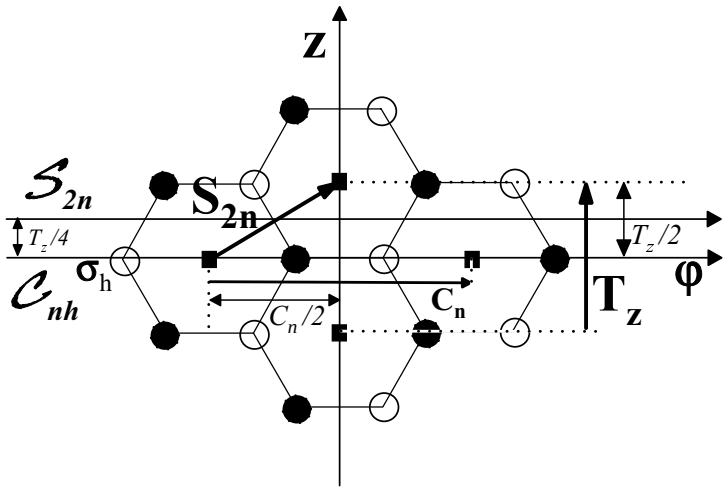

Figure 3: 2D projection of various symmetries in armchair BNT's (•, B; ∘, N): $\mathbf{T_z}$ is the primitive translation; $\mathbf{S_{2n}}$ is the screw axis with non-primitive translation and rotation, denoted by $T_z/2$ and $C_n/2$, respectively; $\mathcal{C}_{nh}|_{z=0}$ and $\mathcal{S}_{2n}|_{z=\frac{T_z}{4}}$ stand for the corresponding point-group operations, among which $\sigma_\mathbf{h}$ and $\mathbf{C_n}$ are denoted. Note the $T_z/4$ shift between $\mathcal{C}_{nh}|_{z=0}$ and $\mathcal{S}_{2n}|_{z=\frac{T_z}{4}}$, that coexist in all armchair BNT's.

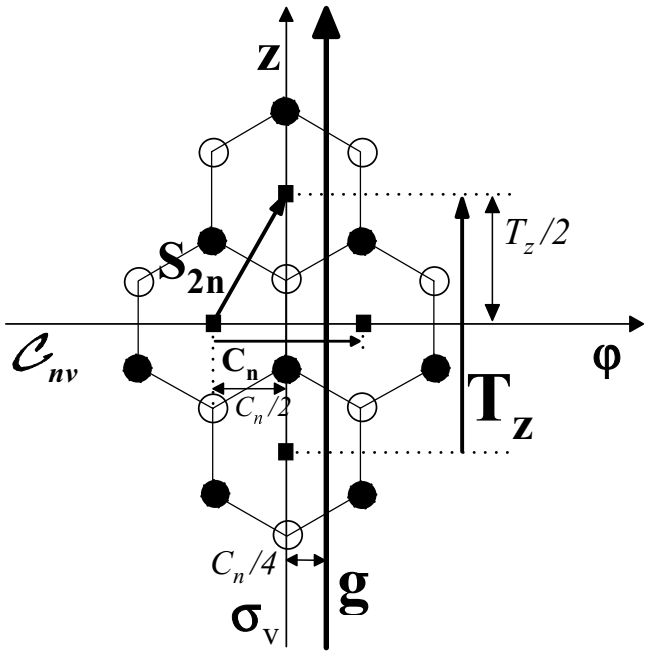

Figure 4: 2D projection of various symmetries of zigzag BNT's (•, B; ∘, N): $\mathbf{T_z}$ is the primitive translation; $\mathbf{S_{2n}}$ is the screw axis with non-primitive translation and rotation, denoted by $T_z/2$ and $C_n/2$, respectively; $\mathbf{g}$ is a glide plane; $\mathcal{C}_{nv}$ stands for the corresponding point-group operations, among which $\sigma_\mathbf{v}$ and $\mathbf{C_n}$ are denoted.

Of these modes, the ones that transform according to $\Gamma_{\rm t} = A_g \oplus E_{1g}^{\pm} \oplus E_{2g}^{\pm}$ (the tensor representation) or $\Gamma_{\rm v}$ are Raman- or IR-active, respectively. Out of the $6N$ phonon modes, four (which transform as $\Gamma_{\rm v}$ and $\Gamma_{R_z} = A_g$) have vanishing frequencies [20]. Consequently, the symmetries and numbers of optically-active phonon modes in armchair BNT's are given by:

$$\Gamma_{\rm Raman}^{arm} = 3A_g \oplus 2E_{1g}^{\pm} \oplus 4E_{2g}^{\pm} \implies n_{\rm Raman}^{arm} = 9\,, \tag{30}$$

$$\Gamma_{\rm IR}^{arm} = A_u \oplus 3E_{1u}^{\pm} \implies n_{\rm IR}^{arm} = 4. \tag{31}$$

Note that the numbers of Raman- and infrared-active phonon modes found for armchair BNT's are almost the same as for armchair CNT'S (8 Raman- and 3 IR-active modes; see Sec. **II**).

Analogously to the treatment given above for armchair BNT's, we would like to discuss the irrep's of $\mathcal{G}_0^{zig}[n] = \mathcal{C}_{2nv}$. Recall that the character table of $\mathcal{C}_{2nv}$ possesses $n+3$ irrep's [19],

$$\Gamma_{\mathcal{C}_{2nv}} = A_1 \oplus A_2 \oplus B_1 \oplus B_2 \oplus \sum_{j=1}^{n-1} E_j. \tag{32}$$

The $6N$ phonon modes transform according to the following irrep's:

$$\Gamma_{6N}^{zig} = \Gamma_{\rm a}^{zig} \otimes \Gamma_{\rm v} = 4A_1 \oplus 2A_2 \oplus 4B_1 \oplus 2B_2 \oplus \sum_{j=1}^{n-1} 6E_j\,, \tag{33}$$

where,

$$\Gamma_{\rm a}^{zig} = 2\left(A_1 \oplus B_1 \oplus \sum_{j=1}^{n-1} E_j\right) \tag{34}$$

and $\Gamma_{\rm v} = A_1 \oplus E_1$. Of these modes, the ones that transform according to $\Gamma_{\rm t} = A_1 \oplus E_1 \oplus E_2$ and/or $\Gamma_{\rm v}$ are Raman- and/or IR-active, respectively. Four of the $6N$ phonon-modes, those which transform as $\Gamma_{\rm v}$ and $\Gamma_{R_z} = A_2$, have vanishing frequencies [20]. Consequently, the symmetries and numbers of optically-active phonon modes in zigzag BNT's are given by:

$$\Gamma_{\rm Raman}^{zig} = 3A_1 \oplus 5E_1 \oplus 6E_2 \implies n_{\rm Raman}^{zig} = 14\,, \tag{35}$$

$$\Gamma_{\rm IR}^{zig} = 3A_1 \oplus 5E_1 \implies n_{\rm IR}^{zig} = 8\,. \tag{36}$$

Note that the numbers of Raman- and infrared-active phonon modes found for zigzag BNT's are almost twice as for zigzag CNT's (8 Raman- and 3 IR-active modes; see Sec. **II**) or armchair BNT's (see Eqs. (30-31)). In addition, as a result of the lowered symmetry with respect to and in contrast to the situation for zigzag CNT's, *all* 8 IR-active modes are Raman-active as well.

B. Chiral boron-nitride nanotubes

Finally, let us discuss the (n,m)-chiral BNT. Following the lack of C_2 axes in $p3m1$, the $\mathcal{D}_d$ point-group in the (n,m)-chiral CNT (see Eq. (16)) reduces to $\mathcal{C}_d$ in the (n,m)-chiral BNT. Nevertheless, the (n,m)-chiral BNT still possesses the non-symmorphic rod-group symmetries, because the screw-axis $\mathbf{S_N}$ "survives" the above symmetry lowering. Consequently, the non-symmorphic rod-group describing the (n,m)-chiral BNT can be decomposed as follows (the first family of rod-groups [17]),

$$\mathcal{G}^{ch}[N] = \mathcal{L}_{T_z} \times \mathcal{C}_d \times \left[\sum_{j=0}^{\frac{N}{d}-1} \mathbf{S}^{\mathbf{j}}_{\frac{\mathbf{N}}{\mathbf{d}}} \right] = \mathcal{L}_{T_z} \times \left[\sum_{j=0}^{N-1} \mathbf{S}^{\mathbf{j}}_{\mathbf{N}} \right] . \tag{37}$$

From Eq. (37) we easily find the point-group of the rod-group,

$$\mathcal{G}_0^{ch}[N] = \mathcal{C}_d \times \left[\sum_{j=0}^{\frac{N}{d}-1} C^j_{\frac{N}{d}} \right] = \sum_{j=0}^{N-1} C^j_N = \mathcal{C}_N . \tag{38}$$

In order to determine the symmetries (at the Γ-point) of the $6N$ phonon modes in chiral BNT's and how many modes are Raman- and/or IR-active we have to associate them with the irrep's of $\mathcal{G}_0^{ch}[N] = \mathcal{C}_N$. Recall that the character table of $\mathcal{C}_N$ possesses N irrep's [19],

$$\Gamma_{\mathcal{C}_N} = A \oplus B \oplus \sum_{j=1}^{\frac{N}{2}-1} E^{\pm}_j . \tag{39}$$

The $6N$ phonon modes transform according to the following irrep's:

$$\Gamma^{ch}_{6N} = \Gamma^{zig}_{\mathrm{a}} \otimes \Gamma_{\mathrm{v}} = 6A \oplus 6B \oplus \sum_{j=1}^{\frac{N}{2}-1} 6E^{\pm}_j , \tag{40}$$

where,

$$\Gamma^{ch}_{\mathrm{a}} = 2 \left(A \oplus B \oplus \sum_{j=1}^{\frac{N}{2}-1} E^{\pm}_j \right) = 2\Gamma_{\mathcal{C}_N} \tag{41}$$

and $\Gamma_{\mathrm{v}} = A \oplus E^{\pm}_1$. Of these modes, the ones that transform according to $\Gamma_{\mathrm{t}} = A \oplus E^{\pm}_1 \oplus E^{\pm}_2$ and/or Γ_{v} are Raman- and/or IR-active, respectively. Four of the $6N$ phonon-modes, those which transform as Γ_{v} and $\Gamma_{R_z} = A$, have vanishing frequencies [20]. Consequently, the symmetries and numbers of optically-active phonon modes are given by:

$$\Gamma^{ch}_{\mathrm{Raman}} = 4A \oplus 5E^{\pm}_1 \oplus 6E^{\pm}_2 \implies n^{zig}_{\mathrm{Raman}} = 15 , \tag{42}$$

$$\Gamma^{ch}_{\mathrm{IR}} = 4A \oplus 5E^{\pm}_1 \implies n^{zig}_{\mathrm{IR}} = 9 . \tag{43}$$

Note that the numbers of Raman- and infrared-active phonon modes found for chiral BNT's are almost the same as for chiral CNT's (14 Raman- and 6 IR-active modes; see Sec. (**II**)).

IV. SUMMARY AND CONCLUSIONS

By utilizing the higher symmetry factor-group $\mathcal{D}_{2nh}$ for the symmetry analysis of phonon modes in achiral CNT's we find that the number of Raman- and IR-active vibrations is about half from what was previously predicted: 8 (Raman) and 3 (IR), rather then 15-16 and 7-8, respectively [4]. This result corroborates the recent experimental results (Rao *et al.* [13], Journet *et al.* [14]) and theoretical predictions (Saito *et al.* [11,12]) of Raman-line intensities for single-walled armchair CNT's. Our findings also allow for the reverse conclusion that vanishing intensities for those vibrational modes previously predicted to be active might indicate that the higher non-symmorphic symmetry is (well) realized in experimental samples of single-walled CNT's. Similarly, by applying the factor-group $\mathcal{D}_N$ for the analysis of optically-active vibrations in chiral CNT's we find that fewer modes are active: 14 (Raman) and 6 (IR), instead of 15 and 9, respectively.

By utilizing the symmetries of the factor-groups $\mathcal{C}_{2nh}$, $\mathcal{C}_{2nv}$ and $\mathcal{C}_N$ we have found that: all armchair BNT's have 9 Raman- and 4 IR-active phonon modes; all zigzag BNT's have 14 Raman- and 8 IR-active phonon modes; all chiral BNT's have 15 Raman- and 9 IR-active phonon modes. Especially and unlike the situation in achiral CNT's, the number of Raman- and infrared-active vibrations in zigzag BNT's is almost twice as in armchair BNT's.

ACKNOWLEDGMENTS

This work is supported in part by the Basic Research Foundation administered by the Israeli Academy of Sciences and Humanities and by the Fund for the Promotion of Research at Technion. The author wishes to thank Prof. N. Moiseyev, Dr. V. Averbukh and Prof. U. Peskin for many helpful discussions and comments. OEA would like to thank the Minerva Foundation for financial support during his stay in Heidelberg.

REFERENCES

[1] S. Iijima, Nature (London) **345**, 56 (1991).

[2] C. Dekker, Physics Today **52** (5), 22 (1999).

[3] M. Terrones, W. K. Hsu, H. W. Kroto and D. R. M. Walton, Top. Curr. Chem. **199**, 189 (1999).

[4] R. Saito, G. Dresselhaus and M. S. Dresselhaus, *Physical Properties of Carbon Nanotubes* (Imperial College Press, London, 1998).

[5] N. G. Chopra, R. J. Luyken, K. Cherrey, V. H. Crespi, M. L. Cohen, S. G. Louie and A. Zettl, Science **269**, 966 (1995).

[6] D. P. Yu, X. S. Sun, C. S. Lee, I. Bello, S. T. Lee, H. D. Gu, K. M. Leung, G. W. Zhou, Z. F. Dong and Z. Zhang, Appl. Phys. Lett. **72**, 1966 (1998).

[7] A. Rubio, J. L. Corkill and M. L. Cohen, Phys. Rev. B **49**, 5081 (1994).

[8] X. Blase, A. Rubio, S. G. Louie and M. L. Cohen, Europhys. Lett. **28**, 335 (1994).

[9] N. G. Chopra and A. Zettl, Solid State Commun. **105**, 297 (1998)

[10] M. Menon and D. Srivastava, Chem. Phys. Lett. **307**, 407 (1999).

[11] R. Saito, T. Takeya, T. Kimura, G. Dresselhaus and M. S. Dresselhaus, Phys. Rev. B **57**, 4145 (1998).

[12] R. Saito, T. Takeya, T. Kimura, G. Dresselhaus and M. S. Dresselhaus, Phys. Rev. B **59**, 2388 (1999).

[13] A. M. Rao, E. Richter, S. Bandow, B. Chase, P. C. Eklund, K. A. Williams, S. Fang, K. R. Subbaswamy, M. Menon, A. Thess, R. E. Smalley, G. Dresselhaus and M. S. Dresselhaus, Science **275**, 187 (1997).

[14] C. Journet, W. K. Maser, P. Bernier, A. Loiseau, M. Lamy de la Chapells, S. Lefrant, P. Deniard, R. Lee, and J. E. Fischer, Nature **388**, 756 (1997).

[15] O. E. Alon, Phys. Rev. B **63**, 201403(R) (2001).

[16] M. Damnjanović I. Milošević, T. Vuković and R. Sredanović, Phys. Rev. B **60**, 2728 (1999); M. Damnjanović I. Milošević, T. Vuković and R. Sredanović, J. Phys. A **32**, 4097 (1999).

[17] M. Damnjanović and M. Vujičić, Phys. Rev. B **25**, 6987 (1982).

[18] J. F. Cornwell, *Group Theory and Electronic Energy Bands in Solids* (North-Holland, Amsterdam, 1969).

[19] D. C. Harris and M. D. Bertolucci, *Symmetry and Spectroscopy: an Introduction to Vibrational and Electronic Spectroscopy* (Dover, NY, 1989).

[20] C. Y. Liang and S. Krimm, J. Chem. Phys. **25**, 543 (1956).

[21] M. Damnjanović, T. Vuković, I. Milošević, and B. Nikolić, Acta Cryst. bf A57, 304 (2001).

[22] O. E. Alon, Phys. Rev. B **64**, 153408 (2001).

[23] P. Král, E. J. Mele and D. Tománek, Phys. Rev. Lett. **85**, 1512 (2000).